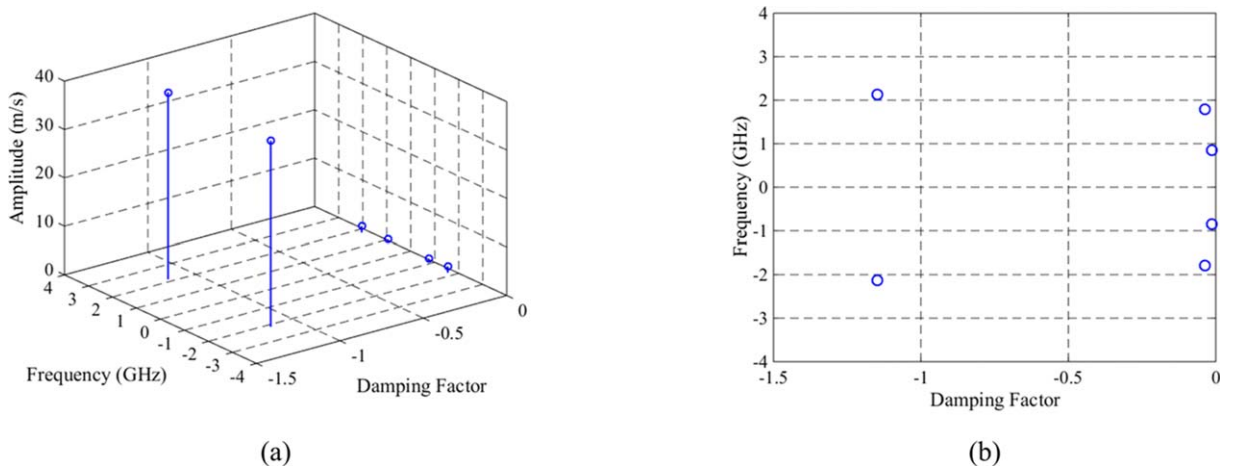

Figure 20 Using the proposed modified MP method, (a) pole-residue relationship (b) location of poles with damping factor. [Color figure can be viewed at wileyonlinelibrary.com]

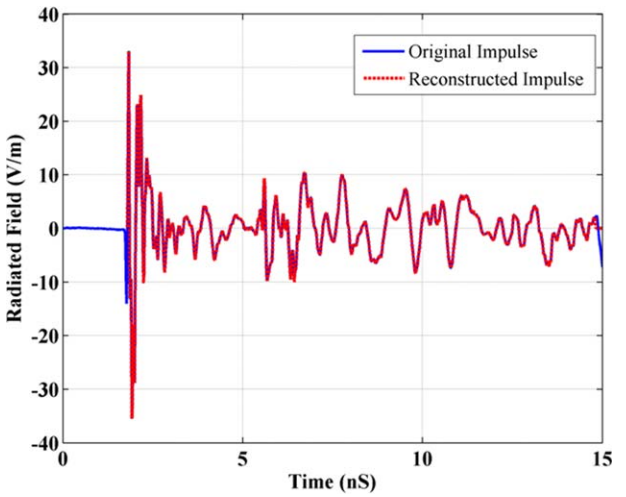

Figure 21 Comparison of the reconstructed and the measured impulse responses for the triple band antenna. [Color figure can be viewed at wileyonlinelibrary.com]

6. CONCLUSION

This article presents system modeling of multiband antennas using the SEM. To acquire the accurate physical complex poles and the corresponding residues of the antenna model in their multiple narrow bands, a modified MP method has been proposed and applied to the impulse response of the antennas. A two-step development to the classical MP is conquered that involves a time segment parameter *TS* to acquire the correct late time response and an adjustable filtering parameter *P* to eliminate the low energy (*E*) nonphysical poles between the multiresonances of the antennas. The poles extracted by the modified MP method are located precisely within the multiple operating bands of each antenna. Three different multiband antennas (dual-band, triple-band, and quad-band antennas) are modeled and their far-field impulse responses are reconstructed and validated using SEM with the proposed MP scheme. A triple band antenna has been fabricated and its far-field impulse response is measured and applied to the proposed MP scheme. The fabricated antenna extracted poles are validated by reconstructing the measured impulse response using the SEM based model.

REFERENCES

1. C.E. Baum, The singularity expansion method: Background and developments, Electromagnetics 1 (1981), 351–360.
2. F. Sarrazin, A. Sharaiha, P. Pouliguen, J. Chauveau, and P. Potier, Helical antenna characterization using the singularity expansion method, In: 2014 IEEE Conference on Antenna Measurements & Applications (CAMA), 2014, pp. 1–4.
3. C.E. Baum, E.J. Rothwell, K.M. Chen, and D.P. Nyquist, The singularity expansion method and its application to target identification, Proc IEEE 79 (1991), 1481–1492.
4. C.E. Baum, Discrimination of buried targets via the singularity expansion, Inverse Probl 13 (1997), 557.
5. S. Licul and W.A. Davis, Unified frequency and time-domain antenna modeling and characterization, IEEE Trans Antennas Propag 53 (2005), 2882–2888.
6. T.K. Sarkar and O. Pereira, Using the matrix pencil method to estimate the parameters of a sum of complex exponentials, IEEE Antennas Propag Mag 37 (1995), 48–55.
7. F. Sarrazin, J. Chauveau, P. Pouliguen, P. Potier, and A. Sharaiha, Accuracy of singularity expansion method in time and frequency domains to characterize antennas in presence of noise, IEEE Trans Antennas Propag 62 (2014), 1261–1269.
8. C.E. Baum, On the singularity expansion method for the solution of electromagnetic interaction problems, DTIC Document 1971.
9. R.S. Aziz, M.A. Alkanhal, and A.F. Sheta, Multiband fractal-like antennas, Prog Electromagn Res B 29 (2011), 339–354.

A NOVEL FAST CLEAN ALGORITHM USING THE GRADIENT DESCENT METHOD

Young-Jae Choi and In-Sik Choi
Department of Electronic Engineering, Hannam University, Daejeon 34430, Korea; Corresponding author: recog@hnu.kr

Received 25 October 2016

ABSTRACT: *An evolutionary programming (EP)-based CLEAN and particle swarm optimization (PSO)-based CLEAN have better accuracy than the FFT-based CLEAN. EP- and PSO-based CLEAN have a higher computational burden, because they must solve a three-dimensional optimization problem using the stochastic search method. To overcome this problem, we employ gradient descent to the CLEAN algorithm. We then compare the performance of the proposed method with that of the PSO-*

based CLEAN and the FFT-based CLEAN. Experimental results show that the proposed algorithm is faster and more accurate than conventional methods. © 2017 Wiley Periodicals, Inc. Microwave Opt Technol Lett 59:1018–1022, 2017; View this article online at wileyonlinelibrary.com. DOI 10.1002/mop.30448

Key words: *CLEAN; evolutionary programming; particle swarm optimization; gradient descent*

1. INTRODUCTION

One-dimensional scattering centers(SCs) are efficient features in radar target recognition. FFT-based CLEAN can extract the SCs in a simple manner. However, FFT-based CLEAN has a resolution limit of 1 Fourier bin (Fbin) [1]. A number of techniques to extract the SC with high resolution have been studied for overcoming the Fbin limitation. The TLS (total least squares)-Prony, matrix-pencil, and generalized eigenvalues utilizing signal subspace eigenvectors (GEESE) methods are commonly used as model-based SC extraction techniques with high resolution [2–4]. These techniques require knowing the number of SCs on the target when extracting the SC. However, estimating the number of SCs of an unknown target is difficult [1]. In 1996, Li et al. proposed a fitting scheme based on the least squares method and a genetic algorithm (GA) for much better accuracy [5]. Although the GA gives much better accuracy, it consumes much more computer time [6]. To overcome this problem, evolutionary programming (EP)-based CLEAN [6] and particle swarm optimization (PSO)-based CLEAN [7] methods are proposed. The computing times of EP and PSO-based CLEAN are less compared to Li et al.'s method [6]. These methods, however, have a limitation in the calculation speed because they must solve a three-dimensional optimization problem using a stochastic search method [6,7].

In this article, we discuss the employment of gradient descent for EP- and PSO-based CLEAN algorithms and a method of reducing the dimensions of the optimization problem. Gradient descent is a well-known method for solving optimization problems. Many related algorithms and applications have been studied [8,9]. Gradient descent must resolve a local minima problem in order to solve the optimization problem. To do so, we utilize the parameters of the SC on a range profile (RP) as the initial value of the optimization problem. We then compare the performance of our proposed method with that of the PSO-based CLEAN. Experimental results show that the proposed algorithm has better performance than that of the PSO-based CLEAN.

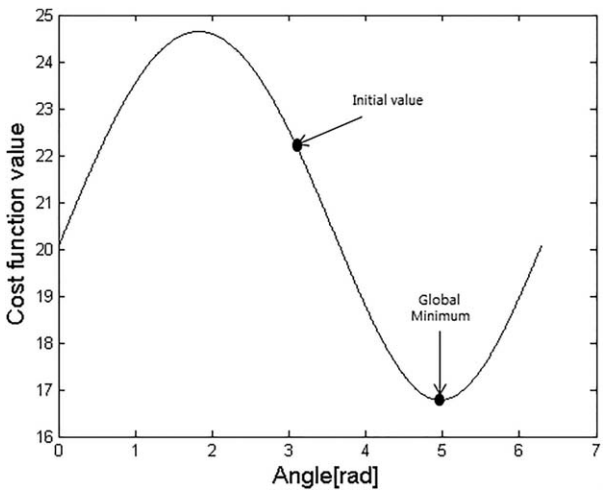

Figure 1 Cost function curve for step 3.

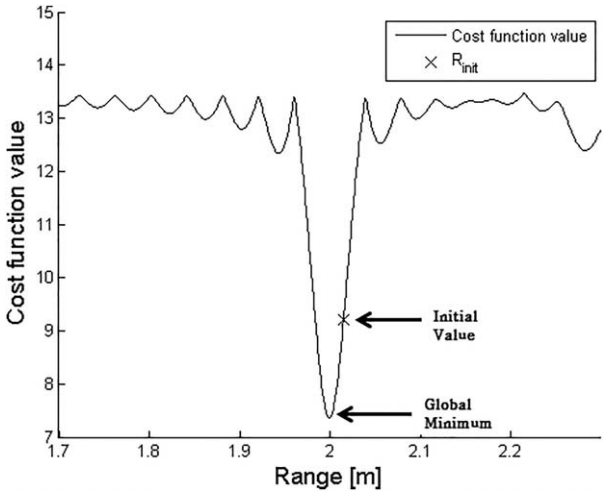

Figure 2 Cost function curve for step 4.

2. PROPOSED CLEAN ALGORITHM

In the proposed CLEAN algorithm, we use the undamped exponential model. According to the undamped exponential model, the scattered field is given by [6]

$$E(f_q)=\sum_{m=1}^{M} a_m \exp\left(-\frac{j4\pi f_q R_m}{c}\right),\ q=1,\cdots,Q, \tag{1}$$

where f_q is the frequency, R_m is the location of the mth SC, a_m is the associated amplitude, c is the speed of light, Q is the number of sampled frequency points, and M is the number of SCs [6].

When A is the highest amplitude in the RP and R is the associated location, the complex amplitude a can be represented in polar form as

$$a=A\exp(j\theta) \tag{2}$$

where θ is the phase of the amplitude, and A is the highest amplitude in the RP.

Using Eq. (2) and the cost function of EP-based CLEAN [6], the cost function is rewritten as

$$J_m=\left|E_m(f_q)-A_m\exp\left\{j(\theta_m-\frac{4\pi f_q R_m}{c})\right\}\right|^2 \tag{3}$$

where A_m is the amplitude of the mth SC, and θ_m is the phase of the associated amplitude.

The detailed proposed CLEAN algorithm is as follows:

Step 1. Set $m=1$, where m is the index of the iteration to extract the mth SC.

Step 2. Obtain the RP of $E_m(f_q)$ for $q=1,2,\cdots,Q$, where $E_m(f_q)$ is the scattered field. Set $R_{\text{init}}=R$, $A_{\text{init}}=A$, where A is the highest amplitude in the RP, and R is the associated location.

Step 3. Obtain the θ value that minimizes the J_m of Eq. (3) using gradient descent where $R_m=R_{\text{init}}$, $A_m=A_{\text{init}}$, and the initial value of $\theta_m=\pi$.

Step 4. Obtain the R value that decreases the J_m of Eq. (3) using one step of gradient descent where $\theta_m=\theta$, $A_m=A_{\text{init}}$, and the initial value of R_m is R_{init}. Set $R_{\text{init}}=R$, and repeat step 3 and

TABLE 1 Ranges and Amplitudes of Five Ideal Point Scatterers

Element Number	Range of Scattering Center (m)	Amplitude of Scattering Center
1	1.0	0.2 + j0.3
2	2.0	0.5 + j0.5
3	2.3	1
4	2.335	0.5 + j0.65
5	4.0	0.3 + j0.4

step 4 until J_m is minimized. If J_m is minimized, set $R_m=R$ and go to step 5.

Step 5. Obtain the A value that minimizes the J_m of Eq. (3) using gradient descent where the initial value of $A_m=A_{\text{init}}$.

Step 6. Obtain $E_{m+1}(f_q)$ by inserting R_m, A_m, and θ_m into Eq. (4):

$$E_{m+1}(f_q)=E_m(f_q)-A_m\exp\left\{j(\theta_m-\frac{4\pi f_q R_m}{c})\right\},\ q=1,\cdots,Q, \quad (4)$$

Step 7. Set $m=m+1$ and return to step 2, unless the desired number of SCs is extracted. We can extract the desired number of SCs by iteration from step 2 to step 6.

The optimization of step 5 does not have the local minima problem in the cost function space. However, the optimization of step 3 and step 4 has a local minima problem. Because gradient descent cannot escape from the local minima, it cannot find the global minima. Fortunately, both cases are problems that can be solved by determining the appropriate initial value. Figure 1 shows the space of the cost function in the case of step 3. It shows that the global minima of θ_m can be obtained by using π as the initial value of θ_m. Figure 2 shows the space of the cost function in the case of step 4. In this case, the initial value of the SC always falls in the global minimum region. Therefore, we can use the gradient descent method in the global region by using R as the initial value of R_m. Because the cost function was converted into polar form, the changes in J_m due to the variable A_m are independent of the variables R_m and θ_m. On the other hand, the changes in J_m due to variable R_m are dependent on the variable θ_m. Therefore, θ_m should be recalculated when R_m is changed.

3. EXPERIMENTAL RESULTS

3.1. Simulation Using Ideal Point Scatterer

In the following experiments, we compare our CLEAN algorithm with two other CLEAN algorithms: FFT-based CLEAN and PSO-based CLEAN. The parameters of the ideal point scatterers used in the simulation are provided in Table 1. The frequency bandwidth ranges from 8.3 to 12.11 GHz at 128 points.

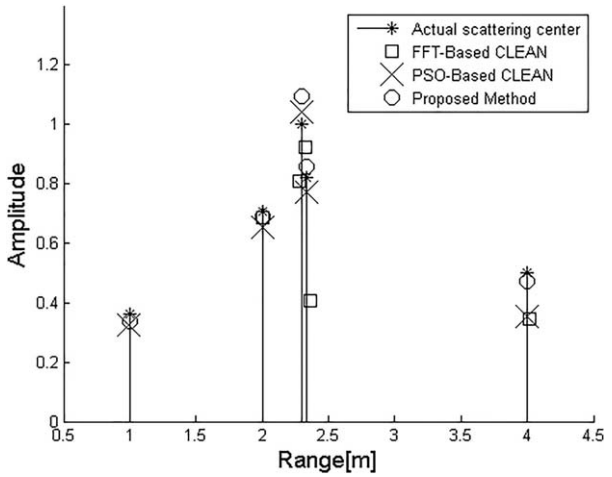

Figure 3 Extracted SCs using each method for SNR = 10 dB when $M=5$.

TABLE 3 Calculation Time for Ideal Point Scatterers with FFT-Based CLEAN, PSO-Based CLEAN, and Proposed CLEAN for SNR = 10 dB

	Extracted Parameters via FFT-Based CLEAN	Extracted Parameters via PSO-Based CLEAN	Extracted Parameters via Proposed CLEAN
Calculation time (s)	0.011	1.727	0.359

We performed simulations using a PC with an Intel Core i3-2120 3.30 GHz dual-core processor. PSO-based CLEAN was performed through 50 generations and 300 particles. Table 2 shows the ranges and absolute amplitudes of the extracted SCs for a signal-to-noise ratio (SNR) of 10 dB. Figure 3 shows that each of the other three algorithms succeeded in extracting the SCs. However, FFT-based CLEAN committed the most errors in regard to both range and absolute amplitude owing to the Fbin problem. PSO-based CLEAN and our proposed CLEAN exhibit better performance in regard to both range and absolute amplitude. Table 3 shows the calculation time for each algorithm. FFT-based CLEAN was faster than the other CLEAN algorithms. On the other hand, PSO-based CLEAN was the slowest because it had to solve the three-dimensional optimization problem using a stochastic search method. The proposed CLEAN method was faster than PSO-based CLEAN because it solved the one-dimensional problem using a gradient descent method. As a result, the proposed CLEAN algorithm achieved both better accuracy and calculation speed.

TABLE 2 Extracted Ranges and Amplitudes (in Parentheses) of Five Ideal Point Scatterers with FFT-Based CLEAN, PSO-Based CLEAN, and Proposed CLEAN for SNR = 10 dB

Element Number	Actual Parameters	Extracted Parameters via FFT-Based CLEAN	Extracted Parameters via PSO-Based CLEAN	Extracted Parameters via Proposed CLEAN
1	1.0000 (0.3606)	2.3622 (0.4057)	0.9920 (0.3561)	0.9990 (0.3373)
2	2.0000 (0.7071)	2.0079 (0.6863)	2.0055 (0.6550)	1.9997 (0.6918)
3	2.3000 (1.0000)	2.2835 (0.8100)	2.2954 (1.0428)	2.3012 (1.0937)
4	2.3350 (0.8201)	2.3228 (0.9235)	2.3342 (0.7712)	2.3383 (0.8594)
5	4.0000 (0.5000)	4.0157 (0.3460)	3.9978 (0.3548)	3.9987 (0.4731)

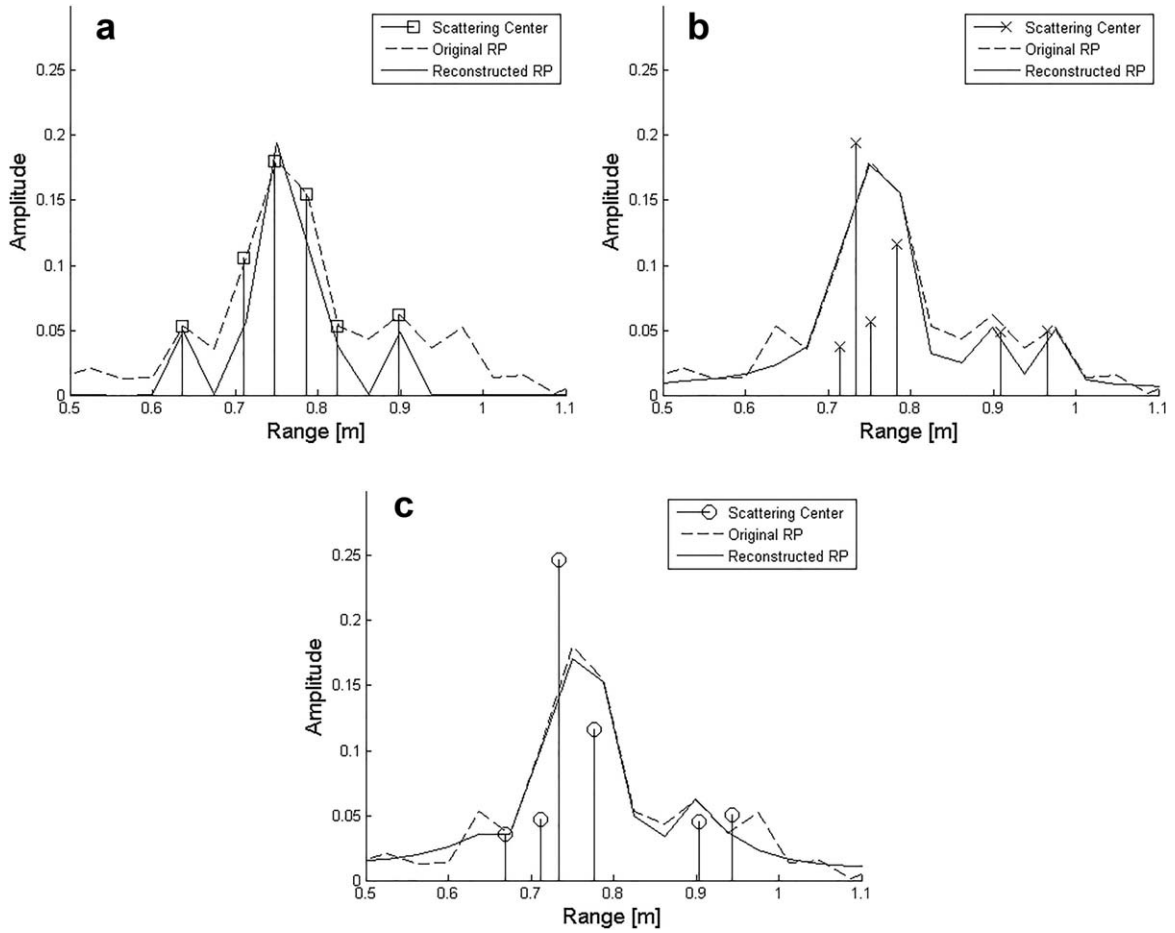

Figure 4 Extracted SCs and reconstructed RP using each method for SNR = 10 dB when $M=6$. (a) FFT-based CLEAN, (b) PSO-based CLEAN, (c) proposed CLEAN.

3.2. Simulation Using Measured Data

To compare the performance of the CLEAN algorithms, we extracted SCs from the scattered data measured using the compact range at the Pohang University of Science and Technology. The measurement frequency is 8.3 to 12.3 GHz with 401 sampling points. The aspect angle is 14.8°, and the elevation angle is 0°. The target used is the 1:16 scaled model of the F-14 Tomcat. Figure 4 is extracted to the SC with each CLEAN method, and the RP reconstructed by the extracted SCs in noise free. Tables 4 and [5] show the result of extracting the SC for SNR = 10 dB. Table 4 shows the relative error (RE) of the reconstructed RP with the original RP. The RE is given by

$$\mathrm{RE}=\frac{\|\mathrm{rp}-\mathrm{rp}'\|_2}{\|\mathrm{rp}\|_2} \tag{5}$$

where rp is the vector of the original RP, rp' is the vector of the RP reconstructed by the SCs extracted with each CLEAN, and $\|\ \|_2$ is the 2-norm. Table 4 shows that the REs of the proposed CLEAN and PSO-based CLEAN are much lower than that of FFT-based CLEAN. Table 5 shows that the computation time of the proposed CLEAN is much lower than that of PSO-based CLEAN, although it is higher than that of FFT-based CLEAN.

TABLE 4 Relative Error of Reconstructed RP with FFT-Based CLEAN, PSO-Based CLEAN, and Proposed CLEAN for SNR = 10 dB

	Extracted Parameters via FFT-Based CLEAN	Extracted Parameters via PSO-Based CLEAN	Extracted Parameters via Proposed CLEAN
Relative error	0.4179	0.1807	0.1511

TABLE 5 Calculation Time for Measured Data with FFT-Based CLEAN, PSO-Based CLEAN, and Proposed CLEAN for SNR = 10 dB

	Extracted Parameters via FFT-Based CLEAN	Extracted Parameters via PSO-Based CLEAN	Extracted Parameters via Proposed CLEAN
Calculation time (s)	0.0180	4.5762	0.4342

4. CONCLUSION

In this article, we proposed a novel CLEAN algorithm for extracting a SC from the one-dimensional RP. The proposed CLEAN algorithm is much faster than PSO-based CLEAN while maintaining the same accuracy. Our CLEAN algorithm can be applied to radar target recognition and to data storage reduction of transient response data. Moreover, it has a noise reduction effect on the RP reconstructed by the SC extracted via the proposed CLEAN algorithm.

ACKNOWLEDGMENTS

This work was supported by the National Research Foundation of Korea (NRF) grant funded by the Korea government (MSIP) (No. 2016R1A2B1011840).

REFERENCES

1. K.T. Kim, and H.T. Kim, One-dimensional scattering centre extraction for efficient radar target classification, IEE Proc Radar Sonar Navigation 146 (1999), 147–158.
2. S.U. Pillai and H.K. Byung, GEESE (GEneralized Eigenvalues utilizing Signal subspace Eigenvectors)—A new technique for direction finding, Twenty-Second Asilomar Conference on Signals Systems and Computers 2 (1988), 568–572.
3. W.M. Steedly, C.J. Ying, and R.L. Moses, Statistical analysis of TLS-based Prony techniques, Automatica 30 (1994), 115–129.
4. Y. Hua, and T.K. Sarkar, Matrix pencil method for estimating parameters for exponentially damped/undamped sinusoids in noise, IEEE Trans Acoust Speech Signal Process 36 (1990), 814–824.
5. Q. Li, E.J. Rothwell, K.M. Chen, and D.P. Nyquist, Scattering center analysis of radar targets using fitting scheme and genetic algorithm, IEEE Trans Antennas Propag (1996).
6. I.S. Choi, and H.T. Kim, Two-dimensional evolutionary programming-based CLEAN, IEEE Trans Aerospace Electron Syst 39 (2003), 373–382.
7. I.S. Choi, Performance comparison of PSO-based CLEAN and EP-based CLEAN for scattering center extraction, Commun Comput Inform Sci 150 (2011), 139–146.
8. L. Mason, J. Baxter, P. Bartlett, and M. Frean, Boosting algorithms as gradient descent, Proc Neural Inform Process Syst (1999), 512–518.
9. C.J.C Burges, T. Shaked, E. Renshaw, A. Lazier, M. Deeds, N. Hamilton, and G. Hulldender, Learning to rank using gradient descent, Proc Int Conf Machine Learn (2005).

SIW-FED VIVALDI ANTENNA WITH BEAM STEERING CAPABILITIES

Jan Puskely,[1] Tomas Mikulasek,[1] Jaroslav Lacik,[1] Zbynek Raida,[1] and Holger Arthaber[2]

[1] Department of Radio Electronics, Brno University of Technology, Brno 616 00, Czech Republic; Corresponding author: puskely@feec.vutbr.cz

[2] Microwave and Circuit Engineering, TU Wien, Institute of Electrodynamics, Vienna 1040, Austria

Received 25 October 2016

ABSTRACT: *A tapered slot antenna element capable of reconfiguring its beam direction is presented. As the basic element, a Vivaldi antenna fed by a substrate integrated waveguide is chosen. The Vivaldi antenna is complemented by a parasitic planar array of small metallic patches placed in front of its aperture and by corrugated edges of the Vivaldi antenna's arms to provide reconfiguration capabilities. The proposed antenna's beam can be steered in five directions by configuring the interconnections of the parasitic patches and by activation/deactivation of the corrugated edges in the antenna arms. The antenna steers the radiation beam over ±30° in* E *plane and operates in the frequency band of 6.0–6.5 GHz. The measured gain at 6.25 GHz for 0°, ±15°, and ±30° beam direction of the antenna with ideal switches, is 8.4 dBi, 7.5 dBi, and 6.7 dBi, respectively.* © 2017 Wiley Periodicals, Inc. Microwave Opt Technol Lett 59:1022–1027, 2017; View this article online at wileyonlinelibrary.com. DOI 10.1002/mop.30447

Key words: *beam steering; reconfigurable antenna; substrate integrated waveguide; Vivaldi antenna*

1. INTRODUCTION

Recent and future high-speed/high-capacity wireless communication systems often demand for high gain, high-efficiency

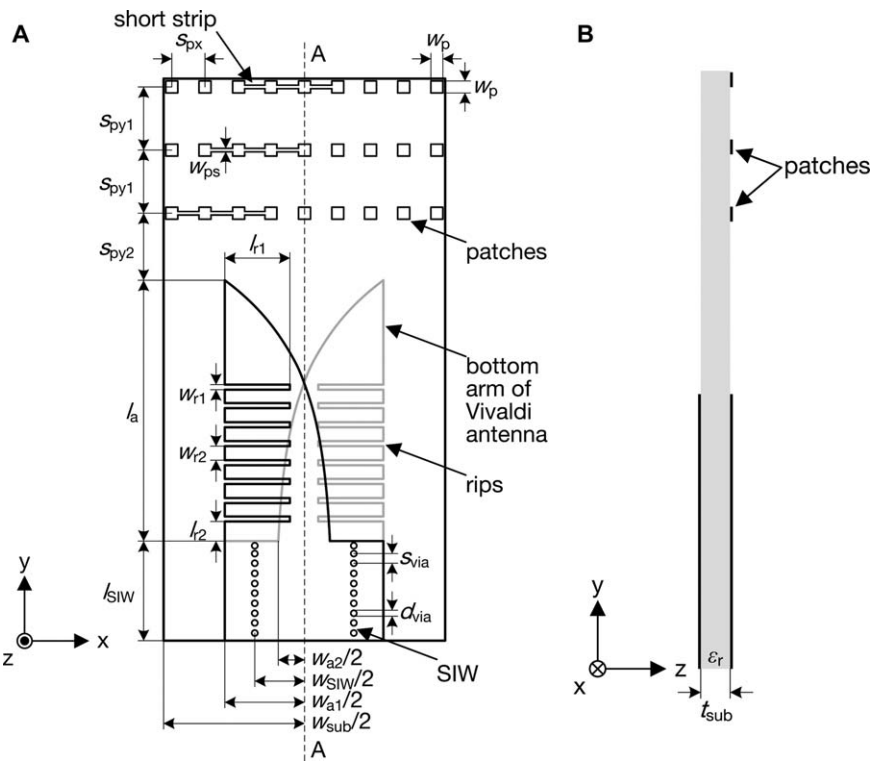

Figure 1 Proposed antenna structure: (a) top view; (b) cross section A–A